

Virtually-enhanced fluid laboratories for teaching meteorology

Lodovica Illari, Department of Earth, Atmospheric and Planetary Sciences, MIT

John Marshall, Department of Earth, Atmospheric and Planetary Sciences, MIT

W. D. McKenna, Department of Earth, Atmospheric and Planetary Sciences, MIT

Corresponding author:

Lodovica Illari

77 Massachusetts Ave

Bldg 54-1612

Cambridge, MA 02143

illari@mit.edu

1 **Abstract**

2 The ‘Weather in a Tank’ project offers instructors a repertoire of rotating tank experiments and a
3 curriculum in fluid dynamics to better assist students in learning how to move between
4 phenomena in the real world and basic principles of rotating fluid dynamics which play a central
5 role in determining the climate of the planet. Despite the increasing use of laboratory
6 experiments in teaching meteorology, many teachers and students do not have access to suitable
7 apparatus and so cannot benefit from them. This article describes a ‘virtually-enhanced’
8 laboratory that could be very effective in getting across a flavor of the experiments and bring
9 them to a wider audience. In the pedagogical spirit of ‘Weather in a Tank’, the focus is on how
10 simple underlying principles, illustrated through laboratory experiments, shape the observed
11 structure of the large-scale atmospheric circulation.

12 **Capsule Summary**

13 A virtually-enhanced 'Weather in a Tank' laboratory illustrates how fundamental principles of
14 rotating fluid dynamics shape the observed structure of atmospheric circulation.

15 **1. Introduction**

16

17 The general circulation of the atmosphere is extraordinarily complex comprising many
18 interacting components. Yet it has an underlying beauty and order which reflects the controlling
19 influence of Earth's rotation and differential heating. At MIT - and in collaboration with other
20 universities (see Illari et al., 2009) - we have explored an approach to teaching meteorology
21 which combines observations with key fundamental theoretical concepts, but which is enlivened
22 and illuminated by carefully chosen rotating laboratory experiments. The importance of
23 laboratory experiments in understanding atmospheric fluid dynamics has been long recognized -
24 Hide (1966), Gill et al. (2010). Persson (2010) stresses how laboratory experiments can help in
25 communicating the non-intuitive nature of geophysical fluids.

26

27 In 'Weather in a Tank' (Illari et al., 2009 and Mackin et al., 2012), the general circulation of the
28 atmosphere emerges from the 'mix' of two key planetary 'ingredients':

29

- 30 1. differential heating of the atmosphere: cooling of polar latitudes relative to the equator
- 31 2. rotation of the earth.

32

33 The first ingredient is intuitively understood and part of common knowledge. However, the
34 second is known to be important but often not well explained, or the details are glossed over.
35 Teachers often believe that rotational effects can only be demonstrated by complex mathematics
36 that are beyond the grasp of many students, particularly in introductory classes (see the
37 discussion in Mackin et al., 2012).

38

39 In 'Weather in a Tank' the combined effect of rotation and differential heating is illustrated using
40 simple laboratory experiments in which a can of ice in the middle of a rotating tank of water
41 represents the Pole-Equator temperature difference and the rotating turntable the rotation of the
42 earth (see Fig.1). A 'three legged stool' approach is followed in which fluid experiments are used
43 together with real time observations and relevant theory (Fig. 1). Students are encouraged to
44 explore the same phenomenon from a number of aspects and become accustomed to moving
45 between observation, theory and laboratory abstraction. The simplification required to set up
46 laboratory experiments demands that complicating details be removed to reveal the essence of
47 the underlying processes at work. This is a truer analogue, we believe, of how research scientists
48 work and, most importantly in the present context, is also very effective pedagogy. Experiments
49 capture the interest of many, if not all students, irrespective of their background knowledge or
50 sophistication in mathematics and physics. They are also great 'fun' and particularly useful in
51 outreach to non-scientists and the public in informal educational settings such as museums and
52 libraries.

53

54 This use of laboratory experiments combined with real world phenomena and relevant theory has
55 proved very effective in teaching the non-intuitive nature of rotating fluids in undergraduate
56 courses. Over the past several years many colleges have adopted the curriculum and the related
57 equipment. A comprehensive guide to the 'Weather in a Tank' experiments and how to obtain
58 the apparatus can be found in Illari and Marshall, (2006). For a quantitative assessment of the
59 impact of the 'Weather in a Tank' curriculum on student learning see Mackin et al., 2012.
60 Despite the increasing use of laboratory experiments in teaching meteorology we are acutely

61 aware that many teachers and students do not have access to suitable apparatus and so cannot
62 benefit from them. However, the digital world of online education provides the possibility of
63 reaching out to a vast audience of ‘distance’ learners. How can we make a laboratory experience
64 available to such an audience? Thus far virtual labs available to the educators in meteorology are
65 mainly comprised of computational modules or educational games – see, for example, the virtual
66 labs from UCAR listed in the references. Here, instead, we describe a ‘virtually-enhanced’
67 laboratory that is very effective in getting across a flavor of the experiments and bringing them to
68 a wider audience. In the pedagogical spirit of ‘Weather in a Tank’ we focus on how simple
69 underlying principles, illustrated through laboratory experiments, shape the observed structure of
70 the large-scale atmospheric circulation.

71

72 Our paper is set out as follows. In Section 2 we describe the teaching method we advocate and
73 the role that real and virtual laboratories can play in it. In Section 3 we present a particular
74 example focusing on the Hadley regime of the tropical atmosphere. ‘Virtually-enhanced’ annulus
75 experiments are presented, available through an accompanying website described in the
76 Appendix, which renders digital recordings of laboratory experiments allowing features of the
77 circulation to be viewed from different angles. Real world applications of the Hadley circulation
78 are presented using advanced graphics (Integrated Data Viewer (IDV) by UNIDATA) to
79 highlight connections to the laboratory experiment. In Section 4 we argue that the availability of
80 virtually-enhanced experiments could allow students to benefit from a laboratory experience
81 even though they may not have access to a real laboratory. Finally we outline some of our future
82 plans.

83

84

85

86 **2. Teaching Meteorology Using Virtual Laboratories**

87

88 We begin by briefly describing three closely related fluid experiments used in our undergraduate
89 courses at MIT to teach students about the general circulation of the atmosphere and the
90 underlying dynamical principles that cause it. This will give the reader a flavor of the
91 pedagogical approach advocated here and the central role that laboratory experiments play in it.

92

93 The set-up in the three experiments is the same and comprises a circular tank of water at the
94 center of which is a can containing a mix of ice and water - Fig. 1. The melting ice extracts heat
95 from the surrounding water at the center of the tank, inducing differential cooling and a
96 circulation, the first ingredient mentioned in the introduction. The only difference between the
97 three experiments is in the second ingredient, the rotation rate, Ω , of the turntable, on which the
98 circular tank sits.

99

100 We carry out the following experiments in turn:

101

102 1. non-rotating, $\Omega = 0$: this is used as our control experiment;

103 2. low rotation, $\Omega = \text{small}$ (less than one revolution per minute, rpm), an analogue of the
104 circulation of the tropical atmosphere, the Hadley circulation;

105 3. high rotation, $\Omega = \text{large}$ (order 6 rpm), an analogue of mid-latitude weather systems (see
106 Section 3.5).

107

108 Experiments two and three involve the use of a rotating turntable with a co-rotating camera (see
109 Fig. 1), which may not be available to the teacher. However, the first experiment can easily be
110 carried out in any classroom on a solid bench using readily available equipment, including an ice
111 can, water tank, colored dyes, etc. The ‘virtual lab’ could then be used to illustrate the two
112 rotating experiments.

113

114 The sequence of three experiments can be presented in one (~ 1.5 to 2 hour) class. Even better,
115 perhaps, they can be broken up in to extended activities spread over several classes with related
116 discussions of the laboratory experiments, theory and study of observations.

117

118 We have found it to be very useful to introduce the experiments to the students through use of a
119 matrix (Fig. 2) printed on a sheet of paper which lays out the experiment in a logical order.

120 Before the experiment is carried our students are encouraged to sketch on the matrix what they
121 think will happen, and share and discuss their predictions with the class. The experiment is then
122 performed before returning to a discussion of student predictions in the context of what actually

123 happened, and why. Relevant theory (for example the thermal wind relation, Ekman layers,

124 conservation of angular momentum as described in Marshall and Plumb, 2008) is developed

125 and/or reviewed to help constrain and inform speculations about what did and did not happen.

126 Finally, meteorological observations are explored in a manner that makes the connection to the
127 laboratory experiments clear.

128

129

130

131 **3. Example of pedagogy: Hadley Circulation**

132

133 **3.1 Laboratory experiments**

134 To give the reader a concrete example, we now describe laboratory experiments that pertain to
135 the Hadley Circulation, real and virtual manifestations, associated theory and exploration of
136 relevant meteorological observations.

137

138 *Non-rotating*

139

140 An initially resting tank of water is differentially cooled by filling a can at its center with a mix
141 of ice and water. The system is not rotating and thus represents our ‘control’ experiment. It is
142 very simple yet encourages students to think about the effect of thermal contrast: where does the
143 cold water in contact with the ice can move and what are the consequences for the ‘general
144 circulation’ in the tank?

145

146 The resulting circulation can be easily visualized by using dye (food coloring) and permanganate
147 crystals, as shown in the photograph in Fig. 2 (bottom-left). The permanganate is particularly
148 useful in indicating flow at the bottom since it sinks in the water column, whereas dye is more
149 nearly neutrally-buoyant and reveals flow interior to the fluid. Cold water sinks near the ice can,
150 flows radially outwards (the pink streaks) inducing water on the periphery to rise at the edge of
151 the tank. To conserve mass, surface waters must move towards the ice can, thus completing the
152 overturning circulation. The resulting circulation is axi-symmetric with predominantly radial

153 (inward and outward) flow. Students are generally ‘comfortable’ with this circulation and can
154 readily rationalize what they see happening. But, now, what happens when we add rotation?

155

156 *Slowly rotating*

157

158 The set-up is exactly the same as the non-rotating case except that now the tank of water sits on a
159 turntable which is rotating very slowly, here at only 1 rpm. The scene is viewed from above via a
160 co-rotating camera, as indicated in Fig. 1. Even though the turntable completes only one rotation
161 in a full 60 seconds, the circulation is strikingly different from the non-rotating experiment.

162 Rotation imparts a ‘winding effect’ on the fluid as revealed by the beautiful corkscrew patterns
163 of the green dye-streaks seen in Fig. 3. Flow at the top is cyclonic (in the same sense of rotation
164 as the tank) but flow at the bottom is anti-cyclonic, as revealed by the pink permanganate streaks
165 - Fig. 3 (top right).

166

167 This circulation pattern is a surprise to almost all students and few are able to predict it. Our
168 mind has difficulty in visualizing and anticipating the effects of rotation. This is perhaps not
169 surprising in view of the fact that Hadley himself did not fully appreciate the effect of rotation on
170 atmospheric flows (see Lorenz, 1967; Marshall and Plumb, 2008).

171

172 In summarizing and reviewing student sketches and observed circulation patterns, we introduce
173 angular momentum principles to rationalize the features of the corkscrew zonal circulation. As in
174 the non-rotating experiment, water in the outer region of the tank is displaced by cold waters
175 flowing outward along the bottom, away from the ice can at the center. It rises and subsequently

176 moves inward at the surface. But now with rotation, contracting rings of fluid associated with
177 inward flow conserve their angular momentum and thus speed up, generating upper-level zonal
178 flow which has the same sense of rotation as the tank (i.e. cyclonic). This flow is analogous to
179 the upper-level atmospheric westerlies, as will become apparent later when meteorological data
180 is analyzed (see Section 3.4).

181

182 On reaching the ice can, the water is cooled, descends and moves outward along the bottom.
183 Rings of fluid expand and begin to circulate in the opposite direction of the turntable, as
184 expected from conservation of angular momentum. As can be seen from the pink streaks in Fig.
185 3 (top-right), flow at the bottom is anti-cyclonic (opposite to the sense of rotation of the tank).
186 The bottom flow is directly analogous to the easterly (trade) winds of the low-latitude Hadley
187 circulation. The accompanying video of the experiment, found on the project website, provides
188 views from the camera above the tank and from another camera viewing the side of the tank.

189

190 In summary, the circulation of the low rotation experiment is not intuitive. Many students have
191 difficulty in visualizing what it is going on and it is not easy to anticipate the impact that rotation
192 has on the fluid.

193

194 **3.2 Virtually-enhanced Hadley example**

195

196 The experiments described above have been recorded, put through a process of virtual
197 enhancement using animation software, and presented for viewing over the web. The capture
198 process involves recording from different angles using top and side cameras in co-rotating and

199 laboratory frames. By combining all of the views together using specialized programs such as
200 ‘Rhinoceros 3d’, it is possible to reconstruct and enhance the 3-dimensional structure of the
201 evolving dyes. The process used to produce the virtually-enhanced video is illustrated in Figs. 4
202 & 5.

203

204 As described in more detail in Appendix A, multi-view images of the experiment from two
205 different cameras (top-view from the co-rotating camera above and side-views from camera in
206 the lab) - Fig. 4 - are processed to produce line contours, turned into volumetric meshes and
207 finally fully rendered surfaces as shown in Fig. 5. For more on the rendering process see
208 Appendix A2. The fully rendered surface looks very realistic and can be viewed from different
209 angles. Students can readily see what is going on in 3 dimensions thus gaining a more complete
210 perspective of the effect of rotation on the fluid motion. The enhancement of the video, and the
211 ability to view it over the web, gives students a vivid impression of the experiment, even though
212 they may never have had the benefit of a first-hand experience. The experiment comes alive as in
213 a PIXAR movie! See the fly-by animation from digitally-enhanced, merged video loops here:
214 <http://lab.rotating.co/#/10>.

215

216 The accompanying website - see <http://lab.rotating.co> allows one not only to inspect pre-
217 recorded experiments but is also designed to give one a feel for how and what it is like to carry
218 out the experiment. Moreover data of flow speeds and temperatures are provided enabling one to
219 quantitatively check dynamical balances that one expects to pertain, as we now go on to explain.

220

221

222 3.3 Associated theory

223

224 The Hadley experiment provides an excellent tutorial for exploring the ‘Thermal Wind’ relation,
225 the theory leg of our stool. As described above, the radial temperature gradient (induced by the
226 ice can and decreasing ‘poleward’) supports zonal motions in the tank, the nature of which
227 depends, inter alia, on the rotation rate. When weakly rotating ($\Omega \lesssim 1$ rpm), we see the
228 development of the thermal wind in the form of a strong ‘eastward’ (i.e., super-rotating) flow in
229 the upper part of the fluid which can be revealed by paper dots floating on the surface. At these
230 low rotation rates the flow is stable to baroclinic instability and laminar motion is observed, as
231 seen in Fig. 5, for example. At higher rotation rates the flow breaks up in to eddying motions
232 analogous to synoptic systems, as described in Section 3.5 below and discussed in detail in
233 Section 7.3.1 of Marshall and Plumb (2008).

234 For an incompressible fluid in cylindrical geometry (with radius, r , increasing outwards), the
235 thermal wind relation is:

$$236 \quad \frac{\partial u}{\partial z} = -1/(f\rho)(\partial\rho/\partial r). \quad \text{Eq. (1).}$$

237 Where f is the Coriolis parameter, ρ is the density and u is the azimuthal speed of the current.

238 Since ρ increases towards the center of the tank, because the water is cold there, ($\partial\rho/\partial r < 0$) then,
239 for positive f , $\partial u/\partial z > 0$. Since u is constrained by friction to be weak at the bottom of the tank,
240 we therefore expect to see $u > 0$ at the top, with the strongest flow at the radius of maximum
241 density gradient. As we have seen, dye streaks clearly show the thermal wind shear - see Fig. 3 -
242 especially near the cold can where the density gradient is strong.

243

244 On the web site that accompanies this article, data are presented of the flow speeds (by tracking
245 particles) and temperature gradients (from thermistors deployed in the tank) existing in the
246 Hadley experiment enabling the thermal wind relation, Eq. (1), to be quantitatively checked – see
247 <http://lab.rotating.co/#/31>.

248

249 **3.4 Connections to the observed Hadley circulation**

250

251 Along with the laboratory experiment we have produced graphical displays using IDV
252 (Integrated Data Viewer, by UNIDATA) that enable one to present meteorological observations
253 in a manner which emphasizes connections to the fluid experiments. Students are encouraged to
254 carry out exactly analogous calculations from meteorological data to check the thermal wind in
255 action for atmospheric flows. Indeed the jet observed in the laboratory experiment is directly
256 analogous to the creation of the subtropical jet by the Hadley circulation, as we now discuss.

257

258 In Fig. 6 (top) NCEP re-analysis climatological winter-mean (DJF) data are used to map the
259 main features of the Hadley circulation and strengthen the connection between the real world and
260 the tank experiment. IDV is a powerful graphical package giving us the tools to go beyond the
261 usual horizontal and vertical sections and explore the 3d structure of the atmosphere. The cyan
262 picks out the tubular surface corresponding to westerly winds aloft. The pink tube highlights
263 easterly winds near the surface. The Arctic ice cap is clearly visible at the surface over the pole.
264 Superimposed is the Northern Hemisphere wintertime Hadley Circulation with the meridional
265 and vertical components of the wind indicated by the arrows. The rendering of the data in this

266 way, Fig. 6 (top), makes the connection with the laboratory experiment, Fig. 6 (bottom), much
267 more immediate and compelling.

268

269 To further emphasize the main features of the observed meridional circulation, zonally averaged
270 fields, as shown in the section in Fig. 6, are plotted separately in Fig. 7. Fig. 7 (bottom) shows
271 the potential temperature (θ in K) and zonal wind (u in m/s) in January. In the troposphere
272 maximum warmth is found south of the equator, consistent with the winter radiative forcing. The
273 north-south potential temperature gradient is small in the tropical region, whereas it is large in
274 middle latitudes - this is the Polar front, marking the edge of the dome of cold polar air. By
275 thermal wind arguments there are strong westerlies at upper levels (in middle latitudes), with
276 weaker easterlies in the lower troposphere (at low latitudes). Fig. 7 (top) shows the vertical and
277 meridional winds. Vertical velocities are large in the tropical band with air rising where it is
278 warm (south of the Equator) and sinking where it is colder in the Northern Hemisphere (around
279 30°N). Meridional winds are directed poleward at upper levels and equatorward at low levels,
280 consistent with rising close to the equator and in the subtropics. Arrows mark the sense of the
281 overturning circulation in the tropical regions. Meridional winds tend to be large in the tropical
282 band and small everywhere else – a clear signal of the Hadley circulation confined to the tropical
283 belt.

284

285 Figs. 6 and 7 together give a summary of the general circulation and illustrate the main features
286 of the Hadley cell in the tropics. The connection between the laboratory flows and the observed
287 Hadley circulation is clearly evident.

288

289

290 **3.5 Baroclinic instability of the thermal wind: the weather regime**

291

292 Following our matrix of experiments shown in Fig. 2, students are encouraged to compare and
293 contrast the low rotation Hadley experiment with exactly the same laboratory set-up but now
294 rotating much more rapidly, Ω large, as shown in Fig. 8 (top). This illustrates dynamics typical
295 of the middle-latitudes. The difference is striking: at a higher rotation rate the axi-symmetric
296 circulation of the Hadley regime breaks down. The flow becomes turbulent and more chaotic;
297 tongues of cold and warm fluids intermingle, sliding one on top of one-another – see Fig. 8
298 (middle). The analogy to the mid-latitude weather systems is very evident by visually comparing
299 with Fig. 8 (bottom), showing the 850 mb temperature over the northern hemisphere for a typical
300 wintertime day. Tongues of warm air move north towards the pole, while cold air vice-versa is
301 moving south towards the equator, equilibrating the Pole-Equator temperature gradient. A video
302 of the high rotation experiment together with observed temperature field can be found at
303 <http://lab.rotating.co/#/eddies>.

304

305 The contrast between the low and high rotation experiments helps one grasp the importance of
306 rotation in shaping weather regimes. Students are amazed to see that the complexity of weather
307 systems can readily be captured by such a transparent rotating fluid experiment with an ice can in
308 the middle and an appropriate rotation rate. Indeed, experiments such as these, known as
309 ‘annulus’ experiments, were fundamental to our understanding of the general circulation of the
310 atmosphere: see Hide (1966) for a comprehensive discussion of relevant laboratory experiments
311 and Lorenz’s (1967) classic review of the general circulation of the atmosphere.

312

313 **4. Discussion and Future plans**

314

315 As demonstrated in the ‘Weather in a Tank’ approach to teaching weather and climate (Illari et
316 al., 2009; Mackin et al., 2012), we believe that student learning is enhanced by being exposed to
317 simple rotating fluid analogues of meteorological (and oceanographic) phenomena. However, we
318 are aware that not everyone has access to rotating turntables, hence the emphasis here on
319 virtually-enhanced experiments which can provide a flavor of the true laboratory. Indeed, we
320 have noted in teaching that the availability of a virtually-enhanced laboratory can deepen
321 understanding by helping students to gain a 3d perspective of the phenomenon studied. This is
322 very clear when studying the general circulation of the atmosphere, whose regimes are rather
323 complex and difficult to unravel. The availability of virtually-enhanced movies and snapshots
324 can help the students appreciate the essence of the phenomena. The ‘virtual lab’ can also be used
325 in conjunction with ‘live’ experiments enabling students to replay and explore again both in and
326 out of class. It is also a valuable and highly effective means to reach larger audiences.

327

328 In conclusion, we would like to contrast the approach presented here to other explorations of
329 digital learning in meteorology. Often the ‘virtual laboratory’ is presented in a gaming context
330 (typically in introductory courses) or a set of computational simulations (in more advanced
331 courses). Indeed the UCAR list of virtual labs (scied.ucar.edu) is dominated by games or simple
332 computational exercises. For example there are several virtual tornadoes:

333

- 334 - the early work of Gallus et al (2006) developing a Virtual Tornadic Thunderstorm,
335 combining data collection and analysis;
- 336 - the more recent and very realistic experience provided by the CUBE theater/lab where
337 one steps in to a virtual recreation of the tornado that hit Oklahoma in 2013, Carstensen
338 (2015);
- 339 - the GEOPod game (Yalda et al., 2012), designed to give a 3d virtual experience to
340 meteorology majors. GEOPod makes use of IDV graphics fly-simulation capabilities and
341 encouraged students to ‘dive in’ and analyze a variety of atmospheric data. Evaluation of
342 student learning showed that the technology was not only visually compelling, but also
343 helped students deepen their understanding of meteorological concepts.

344

345 Such examples demonstrate that technology can indeed give exciting experiences to students.

346 The approach presented here is perhaps a little more conservative, rooted as it is in the ‘tradition’
347 of the laboratory exploration of simplified systems in the spirit of geophysical fluid dynamics.

348 Nevertheless, the artful use of laboratory visualization together with the use of 3d graphics of the
349 real phenomena, as made possible by IDV software, can perhaps give new life to these classic
350 experiments and enthuse a new generation of online students helping them understand the world
351 around them at a deeper level.

352 **Acknowledgments**

353 This study was made possible in part by NSF support through AGS-1338814, ‘FESD Type 1:

354 ‘The impact of the ozone hole on the climate of the Southern Hemisphere’.

355

356

357

358

359

360

361

362

363

364

365

366

367

368

369

370

371

372

373

374

375 **Appendix**

376 The rotating fluid experiment presents a 360-degree rolling view to laboratory observers with
377 each complete rotation of the system. This driving action shapes the dynamic forms of ‘Weather
378 in a Tank’ as well as making them opportune subjects for digital capture and virtualization. Here
379 we outline the processes used to create an enhanced animation from video recordings of the
380 Hadley Cell experiment for a virtual laboratory setting as described in Section 3.2.

381

382 **A1. Building a Viewing Tool**

383 Footage of the experiment from multiple cameras is combined into a synchronized multi-view
384 video. Imagery for a selected tank angle is cued into a 3d modeling environment to create a
385 viewing tool for photogrammetric reconstruction of the fluid forms.

386

387 **Camera Set**

388 Set-up of cameras for recording rotating fluid experiments is illustrated in Fig. A1.1:

389

390 ‘A’ is the camera on-axis overhead, co-rotating with the turntable.

391 ‘B’ is the camera on a tripod in the fixed frame of the lab, capturing the vertical structure of the
392 whole system as it turns.

393 ‘C’ is an additional camera affixed to the turntable, providing a single viewpoint which can be
394 used to check the consistency in camera B’s capture.

395

396

397

398 **Synchronized Imagery**

399 Viewing frames from the various cameras are aligned and scaled to be consistent with one-
400 another, as illustrated in Fig. A1.2. The experiment is sampled at a rate of 12 frames per rotation.

401

402 **Fluid zoetropes**

403 The views from around the system over the course of one period can be used to create a virtual
404 co-rotating viewing tool, similar to the cylindrical image sequence inside a zoetrope – see Fig.

405 A1.3.

406 [Software used: AfterFX » Max MSP / Jitter » Rhinoceros 3d]

407

408 **A2. Animation Tools**

409 Information about the evolution of dye streaks in the co-rotating frame is analyzed with selected
410 view-angle observations from the lab frame to build up a 3d animation of the fluid flows.

411

412 **Mapping evolving dye plumes**

413 We use a modeling technique similar to ‘rotoscoping’, in which live footage is traced over to
414 produce a realistic animation. The overhead features of the dye, Fig. A2.1, are traced into a
415 closed 2d contour. This creates an initial curve matching the observed extent of the dye form,
416 which is then traced back in time until the dye returns to the initial droplet.

417

418 The edges of the stretching 2d dye contour are given depth using elevation data from the tripod
419 camera. A top view together with a pair of perpendicular side views allows us to triangulate the
420 vertical structure of the evolving dye plume.

421

422 **Surface volume mesh**

423 In this phase we move from animated line contours to surfaces: the 3d contours in Fig.A2.1 are
424 surfaced, thickened and turned into a closed mesh as shown in Fig. A2.2. This mesh provides the
425 basis for rendering other properties.

426

427 **Photo realistic rendering**

428 The geometric surfaces created by the multi-angle modeling in Fig. A2.2 can be rendered to
429 resemble real dye surfaces. In our case, the turntable, tank, fluid media, dye tracer, and can of
430 ice are rendered separately and overlaid into co-axially nested systems. Some materials'
431 parameters may be modified to reduce effects of refraction which usually distort the image. The
432 final product can be seen as a continuous form without obstruction from the original tank vessel,
433 as shown in Fig. A2.3. The layer-based animation and rendering can then be staged using
434 dynamic views: in the lab, co-rotating with the tank, or even in the flow, moving in sync with a
435 prominent fluid feature, for example, the super-rotating jet at the free surface. The enhancement
436 allows points of views that would otherwise only be available through complex camera set-ups.
437 For example see following movie: <http://lab.rotating.co/#/10>.

438 [Software used: Max MSP « » Rhinoceros 3d + Bongo + V-ray]

439

440 **A3. Website**

441 Real movie, virtual movies and observations of the Hadley cell are organized in a coherent story
442 in the project website – see <http://lab.rotating.co/>

443

444 **Utilizing the Virtual Lab**

445 The website provides a ‘public view’ into the lab and can be used in various contexts:

- 446 - Web-based presentations for large classes or audiences at meetings - the scripted
447 animations can be used instead of the real experiment, when the use of a turntable is not
448 practical.
- 449 - Classroom environment – students can export the virtual models to a specified coordinate
450 system for analysis and interrelation with world observations or their own run of the
451 experiments.
- 452 - Stand-alone - the virtual rendering of the experiment can be replayed, skipped back, and
453 studied at great length to ‘research’ the real behaviors of the fluid.

454

455 The website brings together the rotating fluid experiment and the real world with a
456 comprehensive discussion of the climatology of the Hadley Cell, visualized with IDV (Integrated
457 Data Viewer by Unidata) - see <http://lab.rotating.co/#/world>. Three dimensional plots of the
458 Hadley Cell from climatological data (NCEP reanalysis I) show close analogies to the low
459 rotation tank experiment.

460

461 **Navigation of the website**

462 Visitors to the virtual laboratory will arrive with differing intents, time constraints, and levels of
463 familiarity with the material or laboratory methods. In consideration of this, we have devised a
464 streamlined experience for ‘Weather in a Tank’ watchers along the top-level (progressing by
465 right arrow / left swipe), while elaborations on a subject are folded-in below (discoverable
466 through a downward arrow / upward swipe). We recommend a first pass through the main stream

467 at the top before making a second pass to review and explore in-depth. Jumps across sections are
468 possible on-click of the progress bar which us always present at the bottom, or by revealing the
469 ‘guide’ with the menu icon just above.

470 **References**

471 Carstensen. L. W., 2015: Step into a 3D tornado and see an epic storm up close. *New Scientist*,
472 accessed 23 March 2015. [Available online at [https://www.newscientist.com/article/dn27228-](https://www.newscientist.com/article/dn27228-step-into-a-3d-tornado-and-see-an-epic-storm-up-close)
473 [step-into-a-3d-tornado-and-see-an-epic-storm-up-close.](https://www.newscientist.com/article/dn27228-step-into-a-3d-tornado-and-see-an-epic-storm-up-close)]

474

475 Gallus, W. A., C. Cervato, C. Cruz-Neira, and G. Faidley, 2006: A virtual tornadic thunderstorm
476 enabling students to construct knowledge about storm dynamics through data collection and
477 analysis. *Adv. Geosci.*, **8**, 27–32, doi:10.5194/adgeo-8-27-2006.

478

479 Gill, M., P. Read and L. Smith, 2010: Geophysical flows as dynamical systems: the influence of
480 Hide's experiments. *A&G*, **51** (4): 4.28-4.35. doi: 10.1111/j.1468-4004.2010.51428.x.

481

482 Hide, R., 1966: The dynamics of rotating fluids and related topics in geophysical fluid dynamics.
483 *Bull. Amer. Meteorol. Soc.*, **47**, 873-885.

484

485 Illari, L., and J. Marshall, 2006: Weather in a Tank: A Laboratory Guide to Rotating Tank Fluid
486 Experiments and Atmospheric Phenomena. Accessed 23 March 2015. [Available online at
487 [http://paoc.mit.edu/labguide.](http://paoc.mit.edu/labguide)]

488

489 Illari, L., and Coauthors, 2009: “Weather in a Tank”—Exploiting Laboratory Experiments in the
490 Teaching of Meteorology, Oceanography, and Climate. *Bull. Amer. Meteor. Soc.*, **90**, 1619-1632,
491 doi:10.1175/2009BAMS2658.1.

492

493 Lorenz, E. N., 1967: *The Nature and Theory of the General Circulation of the Atmosphere*.
494 World Meteorological Organization, 161 pp.
495
496 Mackin, K.J., Cook-Smith, N., Illari, L., Marshall, J., and P. Sadler, 2012: The Effectiveness of
497 Rotating Tank Experiments in Teaching Undergraduate Courses in Atmospheres, Oceans, and
498 Climate Sciences. *Journal of Geoscience Education*: **60**, 67-82, doi:10.5408/10-194.1.
499
500 Marshall, J., and R. A. Plumb, 2008: *Atmosphere, Ocean, and Climate Dynamics: An*
501 *Introductory Text*. Academic Press, 319 pp.
502
503 Persson, A. (2010), Mathematics versus common sense: the problem of how to communicate
504 dynamic meteorology. *Met. Apps.*, **17**: 236–242. doi:10.1002/met.205
505
506 UCAR Center for Science and Education, 2012: Games & Simulations about Weather, Climate
507 & the Atmosphere. Accessed 23 March 2015. [Available online at
508 <http://scied.ucar.edu/node/911>.]
509
510 Unidata, 2012: Integrated Data Viewer (IDV) version 3.1. UCAR, accessed 23 March 2015.
511 [Available online at <http://www.unidata.ucar.edu/software/idv/>.]
512
513 Yalda, S., Zoppetti, G., Clark, R., and K. Mackin, 2012: Interactive Immersion Learning: Flying
514 through Weather Data onboard the GEOpod. *Bull. Amer. Meteor. Soc.*, **93**, 1811–1813,
515 doi:10.1175/BAMS-93-12-1811.

516 **Figure captions**

517 Fig. 1. The ‘three-legged-stool’ approach to teaching the fundamentals of atmospheric dynamics
518 at the heart of the ‘Weather in a Tank’ project.

519

520 Fig. 2. Matrix used in teaching the general circulation. Three experiments are carried out in
521 which a radial temperature gradient is induced through use of an ice can, placed at the center of a
522 cylindrical tank of water. The only difference between them is that the rotation rate, Ω , of the
523 tank is different ($\Omega = 0$, small, large).

524

525 Fig. 3. The low rotation ‘Hadley’ experiment: (top) Overhead view shows the evolving
526 azimuthal circulation at early (left) and later (right) times. The pink plume on the right emanates
527 outward from crystals of permanganate dissolving at the bottom of the tank. They indicate the
528 sense of the flow near the bottom. (bottom) Side views show the green dye streaks being tilted
529 over into a corkscrew pattern early (left) and later (right) in the experiment.

530

531 Fig. 4. Views from three mutually perpendicular camera angles provide a spatial fix on the dye
532 plume as it evolves and deforms with the fluid flow. Overhead lineaments are coordinated with
533 side-views of tracer extents, enabling the 3d structure of the plumes to be reconstructed.

534

535 Fig. 5. Rendered (virtual) view of the Hadley Experiment showing the ‘winding up’ of green dye
536 plumes by the cyclonic (anticlockwise viewed from above) flow in thermal wind balance with
537 the radial temperature gradient. The evolution of the anti-cyclonic (clockwise) flow at the bottom
538 is revealed by the pink plume. The geometric surfaces created by the multi-angle views of Fig. 4

539 have been given visual-perceptual properties, which resemble real dye surfaces. The final image
540 is continuous without obstruction of the tank used in the experiment.

541

542 Fig.6. (top) Climatological winter mean circulation, showing upper level westerlies (cyan
543 isosurface of $u = 30$ m/s) and low level easterlies (pink isosurface of $u = -10$ m/s). The meridional
544 section on the left hand side shows the zonally averaged overturning circulation at low latitudes -
545 vertical and meridional wind directions are marked by white arrows. (All fields are plotted using
546 IDV software). (bottom) A schematic diagram of the laboratory Hadley circulation, showing
547 similar features to the observed climatology: the green streak of ‘westerlies’ and the pink plume
548 of surface ‘easterlies’. (cf Fig. 5.)

549

550 Fig. 7. The observed mean meridional circulation during January (from NCEP/NCAR Reanalysis
551 I). (top) Zonally averaged meridional wind (scale on top) and vertical wind (scale on side) are
552 contoured (and colored) and the sense of the flow indicated by arrows. (bottom) Zonally
553 averaged potential temperature (scale on left hand side) and zonal wind (scale on top). Westerly
554 winds are blue-green: easterlies are red-pink. All fields are plotted using IDV software.

555

556 Fig. 8. The high rotation experiment showing baroclinic instability: (top) view from the co-
557 rotating camera showing turbulent eddies transfer fluid from the warm (red) edge of the tank to
558 the cold (green) inner can with ice; (middle) sections across the whole tank, showing the colder
559 green water sliding under the warmer red water and mixing laterally and vertically; (bottom) 850
560 mb temperature on a typical winter day over the North America sector, showing a burst of cold

561 arctic air being advected south over Canada and the US, while a tongue of warm tropical air is
562 advected north.

563

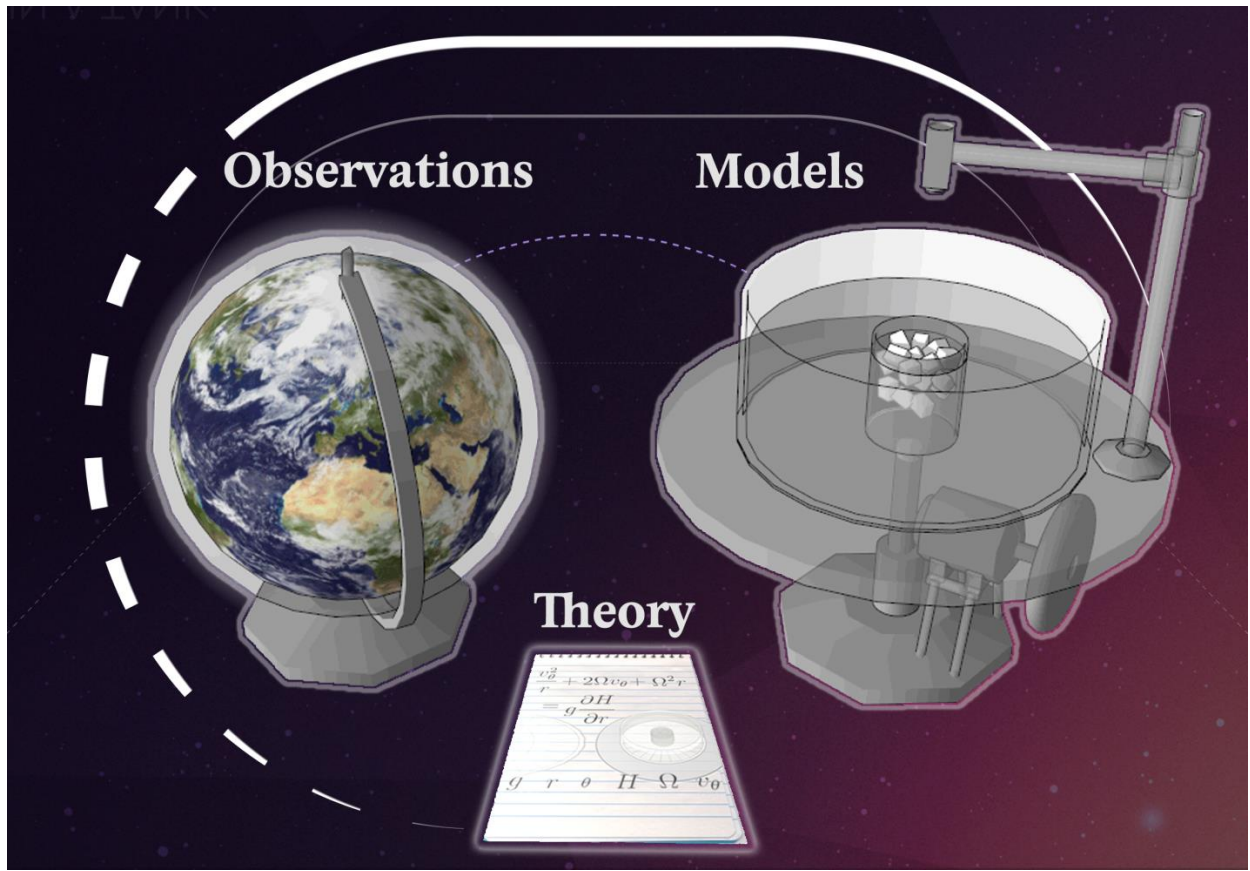
564 Fig. A1. Variable-angle video from a turntable experiment in the lab (1.1) is sampled at a regular
565 frequency subdividing the rotation period (1.2) and mapped to frames linked to time-points of
566 view in the animation environment (1.3).

567

568 Fig. A2. Projections of extracted features from overhead & side-views combine to map the
569 volume of fluid containing dye (2.1). The interpolated contour bounding the evolving dye plume
570 is surfaced (2.2), to produce a visualization of the circulation pattern (2.3).

571

572



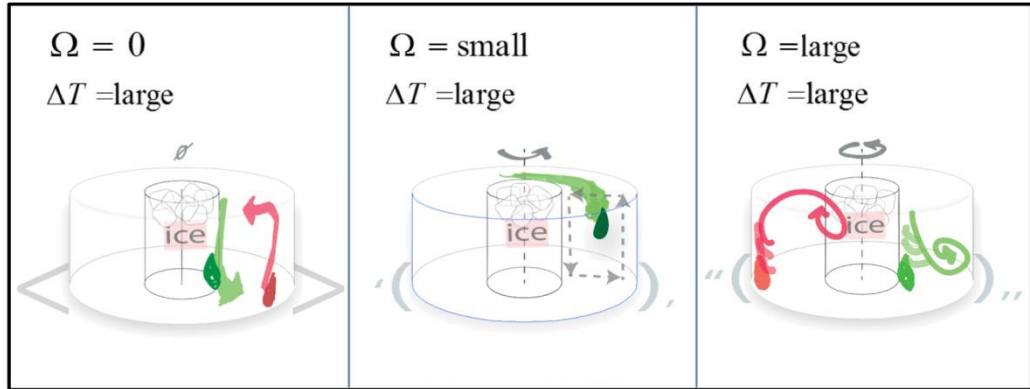
573

574 Fig. 1. The 'three-legged-stool' approach to teaching the fundamentals of atmospheric dynamics

575 at the heart of the 'Weather in a Tank' project.

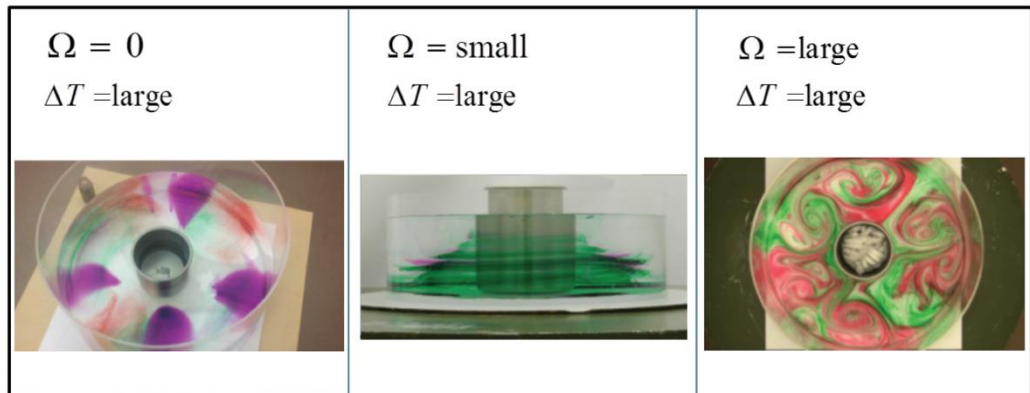
Before

Sketch what you are expecting the flow to look like



After

Sketch the flow you observe



576

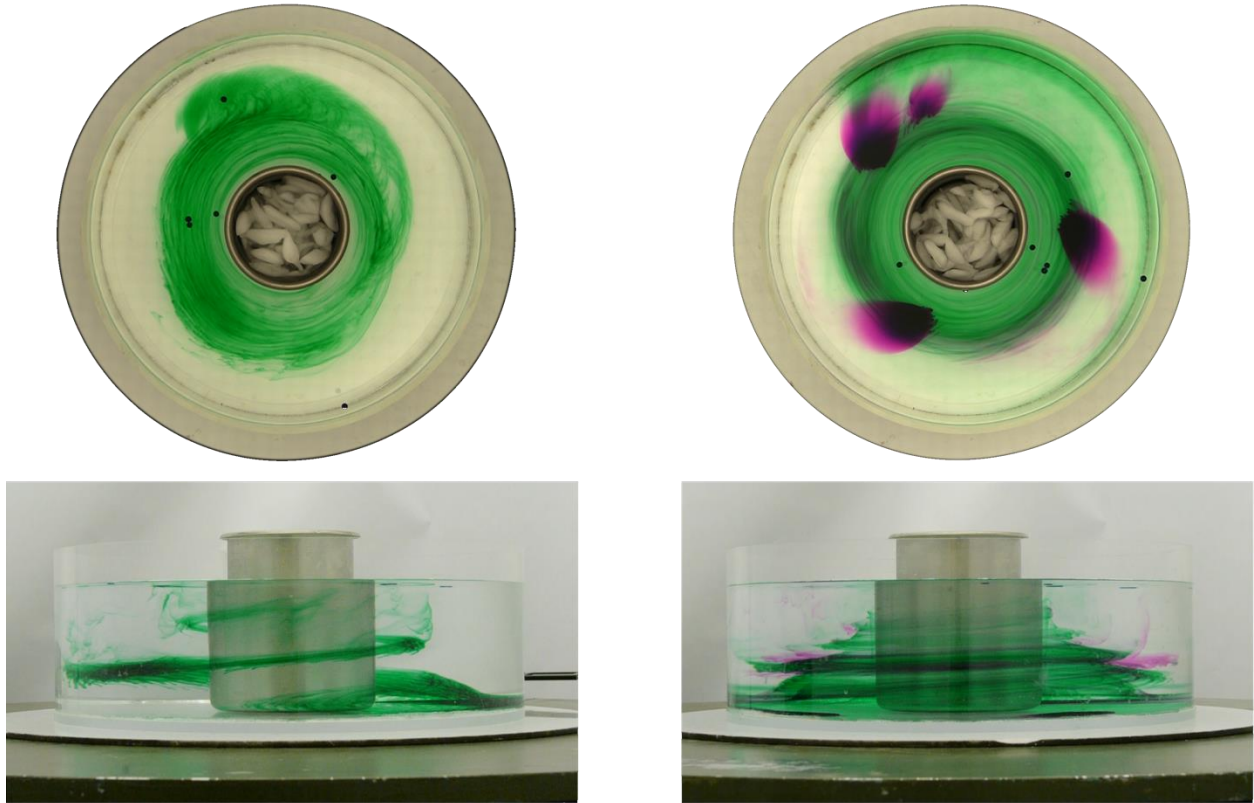
577

578

579

580

Fig. 2. Matrix used in teaching the general circulation. Three experiments are carried out in which a radial temperature gradient is induced through use of an ice can, placed at the center of a cylindrical tank of water. The only difference between them is that the rotation rate, Ω , of the tank is different ($\Omega = 0$, small, large).



581

582

583

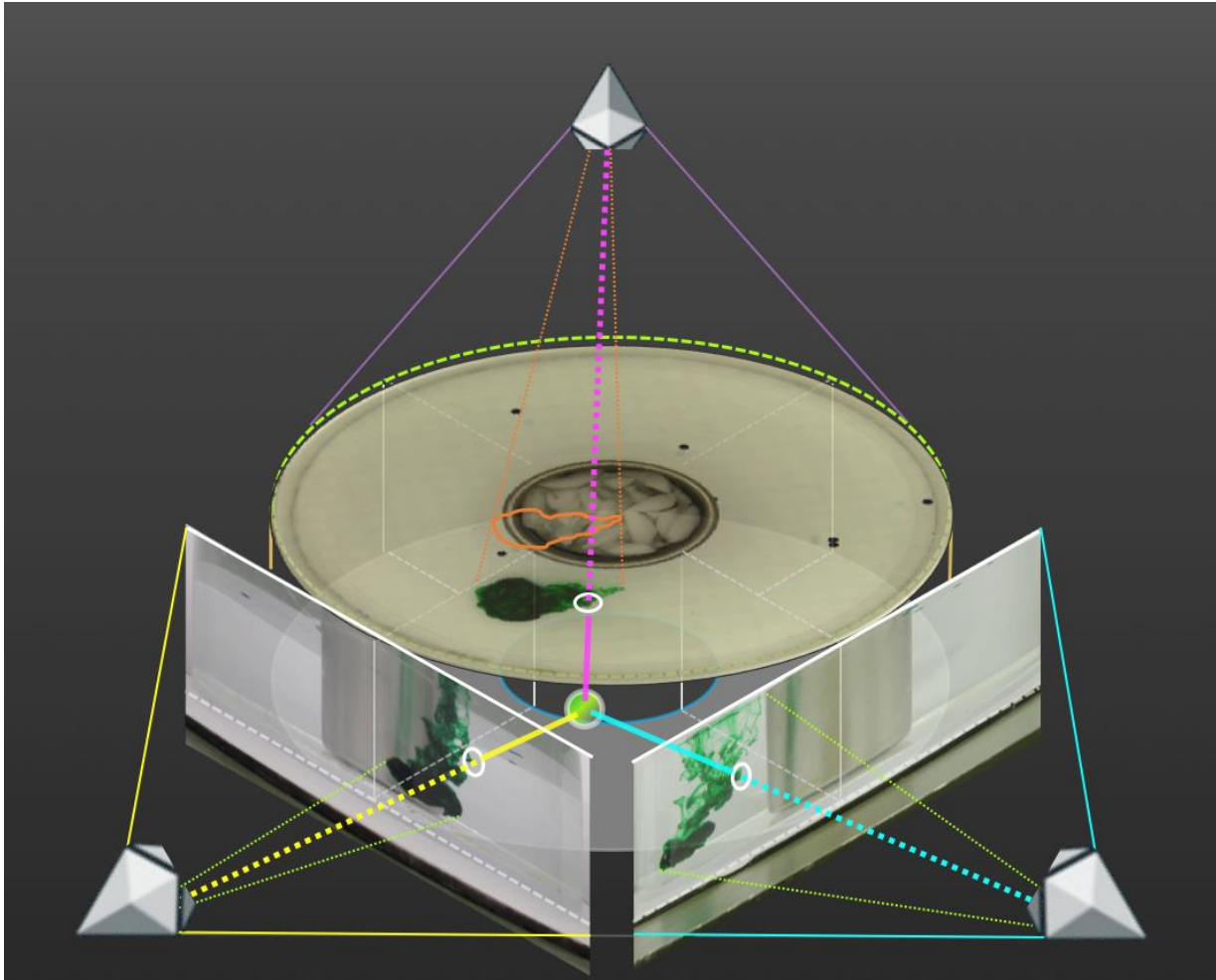
584

585

586

587

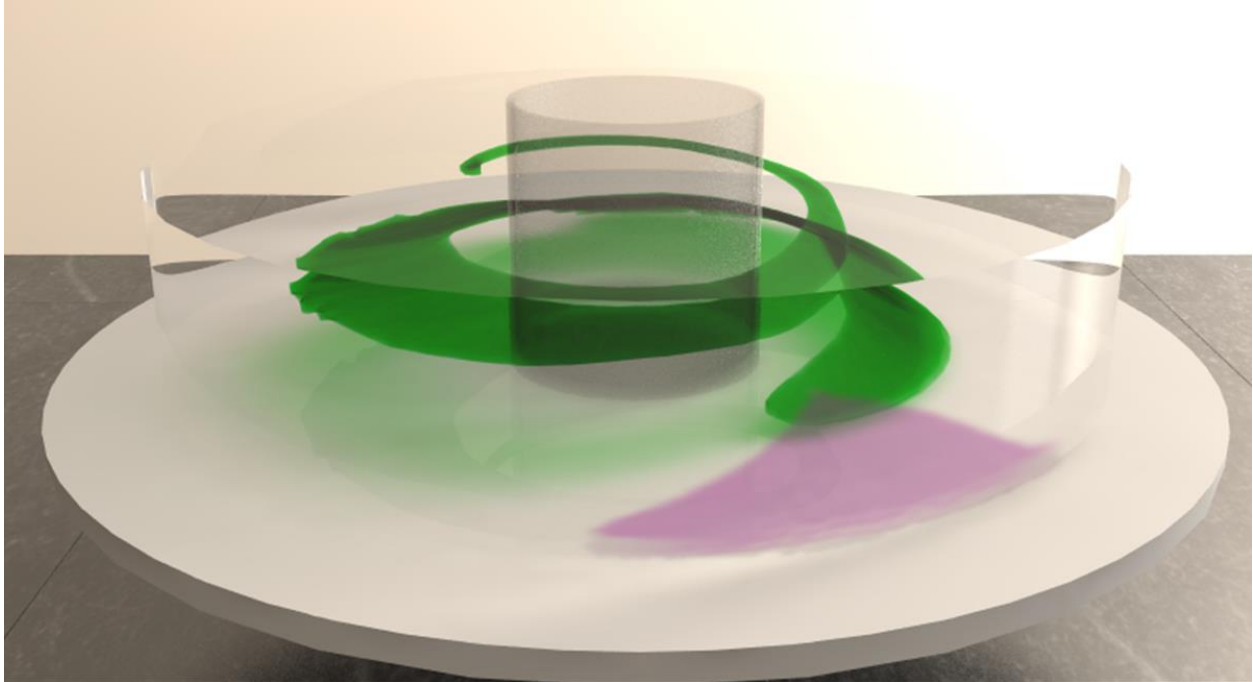
Fig. 3. The low rotation ‘Hadley’ experiment: (top) Overhead view shows the evolving azimuthal circulation at early (left) and later (right) times. The pink plume on the right emanates outward from crystals of permanganate dissolving at the bottom of the tank. They indicate the sense of the flow near the bottom. (bottom) Side views show the green dye streaks being tilted over into a corkscrew pattern early (left) and later (right) in the experiment.



588

589 Fig. 4. Views from three mutually perpendicular camera angles provide a spatial fix on the dye
590 plume as it evolves and deforms with the fluid flow. Overhead lineaments are coordinated with
591 side-views of tracer extents, enabling the 3d structure of the plumes to be reconstructed.

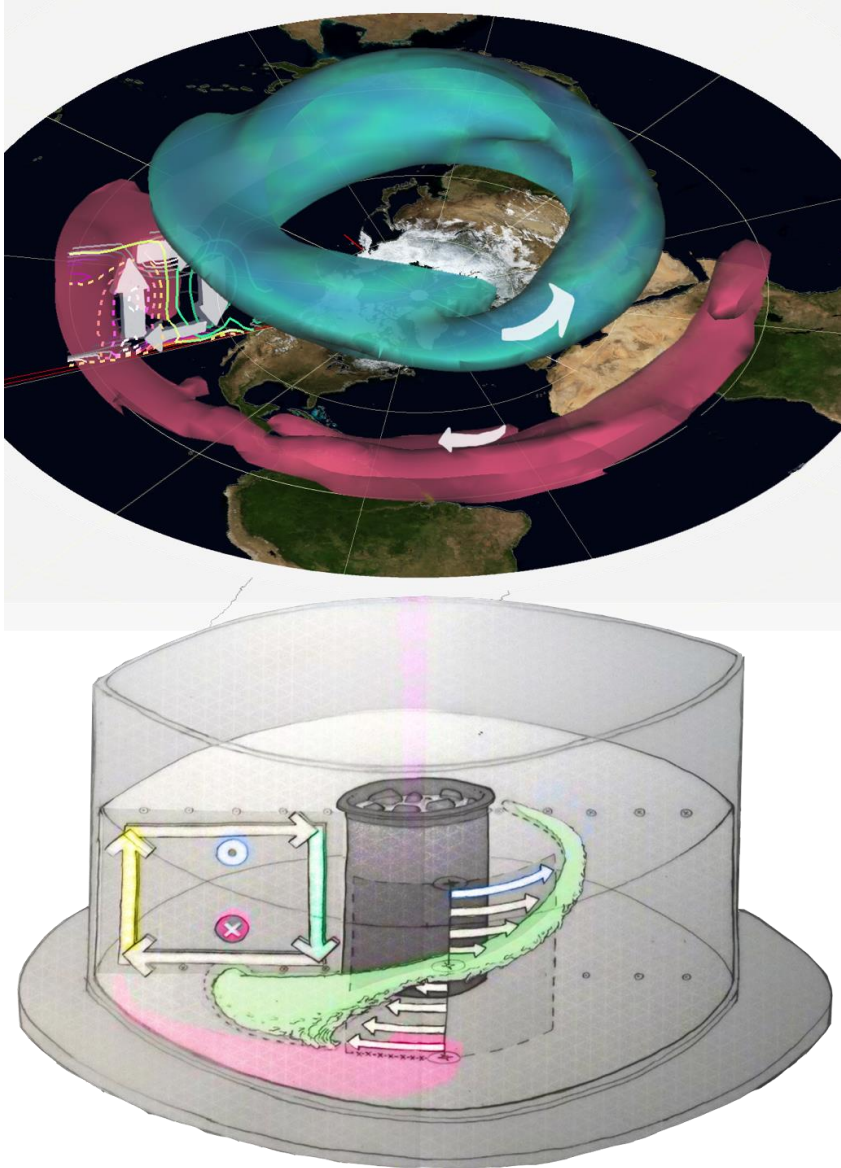
592



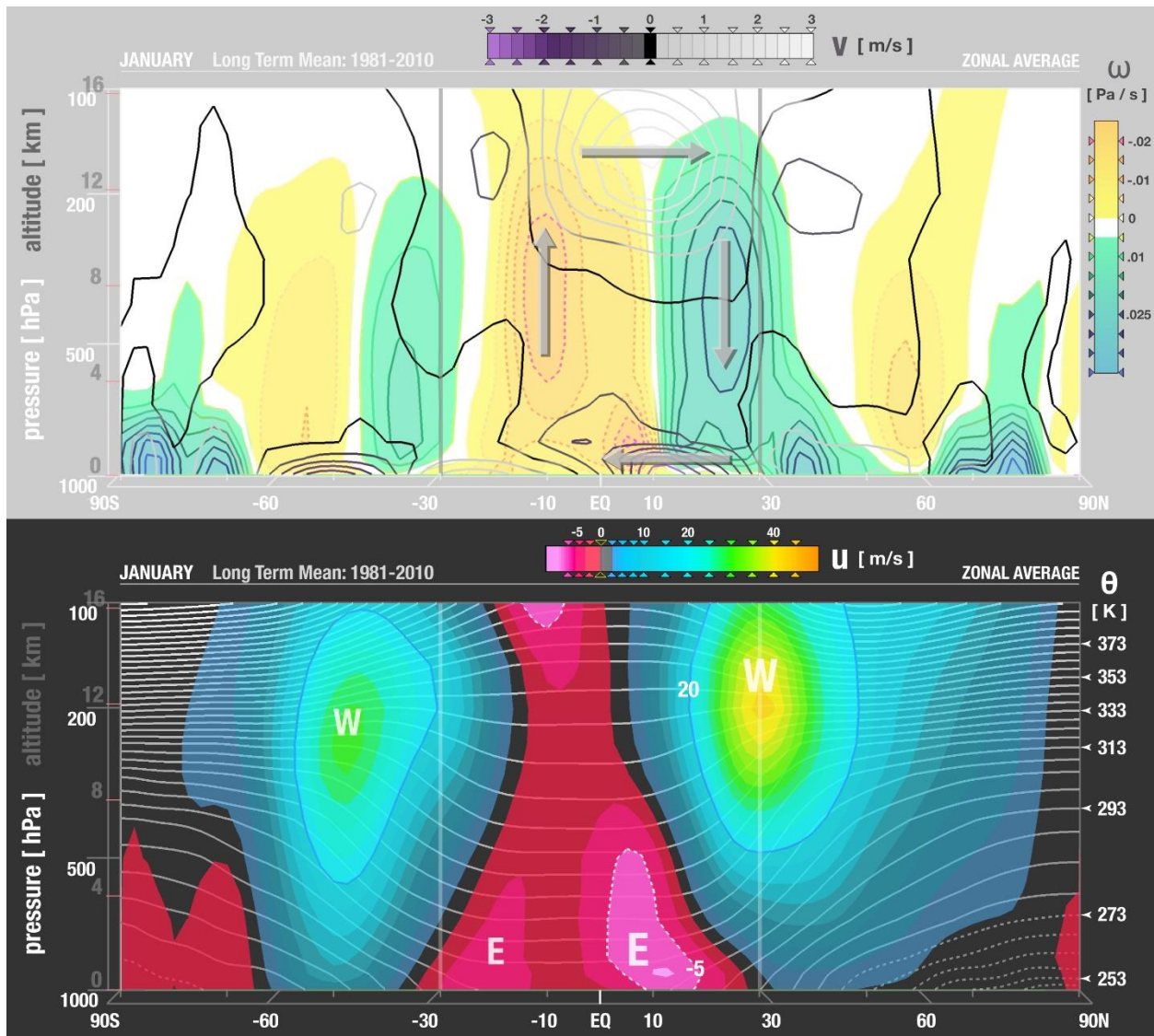
593

594 Fig. 5. Rendered (virtual) view of the Hadley Experiment showing the ‘winding up’ of green dye
595 plumes by the cyclonic (anticlockwise viewed from above) flow in thermal wind balance with
596 the radial temperature gradient. The evolution of the anti-cyclonic (clockwise) flow at the bottom
597 is revealed by the pink plume. The geometric surfaces created by the multi-angle views of Fig. 4
598 have been given visual-perceptual properties, which resemble real dye surfaces. The final image
599 is continuous without obstruction of the tank used in the experiment.

600



601
 602 Fig.6. (top) Climatological winter mean circulation, showing upper level westerlies (cyan
 603 isosurface of $u = 30$ m/s) and low level easterlies (pink isosurface of $u = -10$ m/s). The meridional
 604 section on the left hand side shows the zonally averaged overturning circulation at low latitudes -
 605 vertical and meridional wind directions are marked by white arrows. (All fields are plotted using
 606 IDV software). (bottom) A schematic diagram of the laboratory Hadley circulation, showing
 607 similar features to the observed climatology: the green streak of 'westerlies' and the pink plume
 608 of surface 'easterlies'. (cf Fig. 5.)



609

610 Fig. 7. The observed mean meridional circulation during January (from NCEP/NCAR Reanalysis

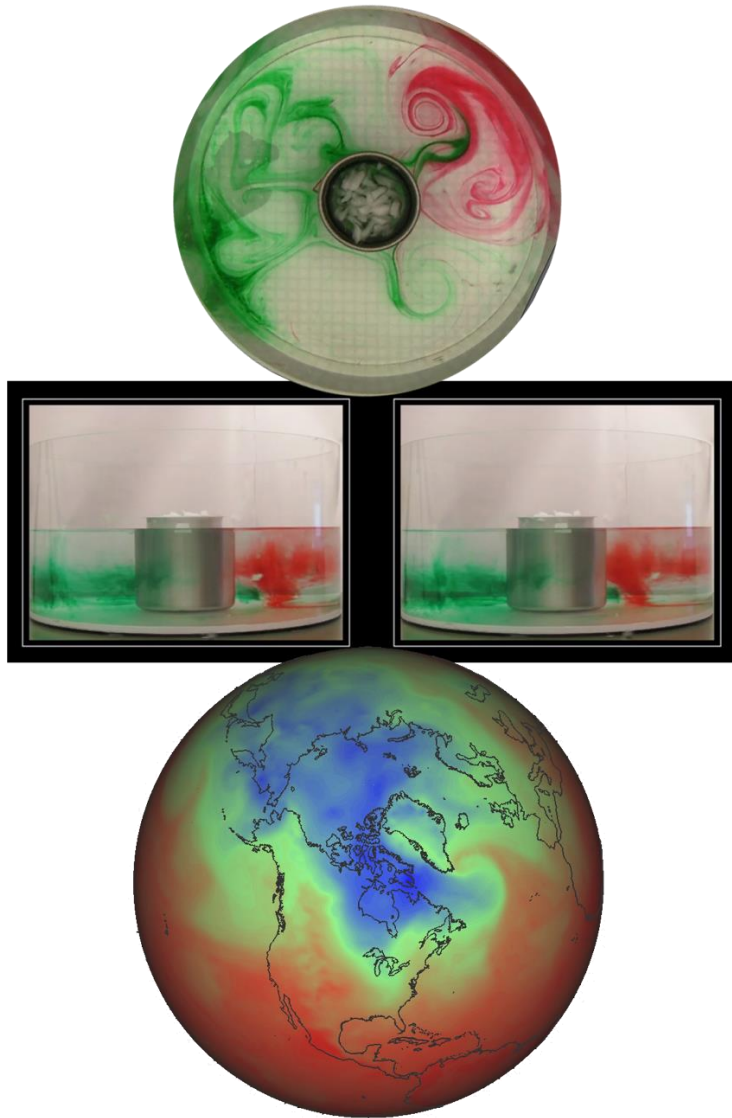
611 I). (top) Zonally averaged meridional wind (scale on top) and vertical wind (scale on side) are

612 contoured (and colored) and the sense of the flow indicated by arrows. (bottom) Zonally

613 averaged potential temperature (scale on left hand side) and zonal wind (scale on top). Westerly

614 winds are blue-green: easterlies are red-pink. All fields are plotted using IDV software.

615

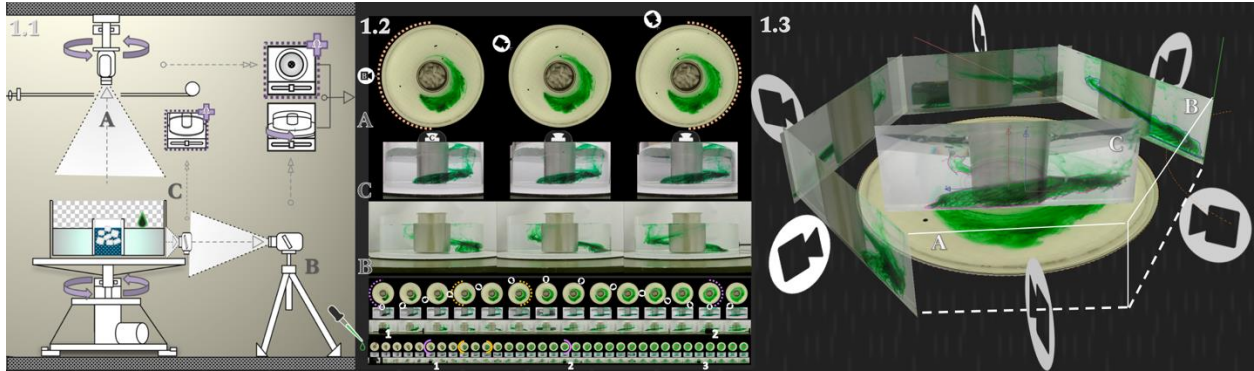


616

617 Fig. 8. The high rotation experiment showing baroclinic instability: (top) view from the co-
618 rotating camera showing turbulent eddies transfer fluid from the warm (red) edge of the tank to
619 the cold (green) inner can with ice; (middle) sections across the whole tank, showing the colder
620 green water sliding under the warmer red water and mixing laterally and vertically; (bottom) 850
621 mb temperature on a typical winter day over the North America sector, showing a burst of cold
622 arctic air being advected south over Canada and the US, while a tongue of warm tropical air is

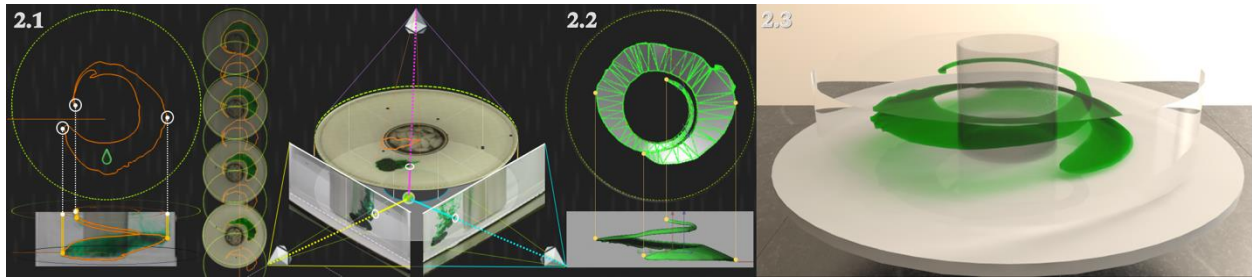
623 advected north.

624



625 Fig. A1. Variable-angle video from a turntable experiment in the lab (1.1) is sampled at a regular
626 frequency subdividing the rotation period (1.2) and mapped to frames linked to time-points of
627 view in the animation environment (1.3).

628



629

630

631

632

Fig. A2. Projections of extracted features from overhead & side-views combine to map the volume of fluid containing dye (2.1). The interpolated contour bounding the evolving dye plume is surfaced (2.2), to produce a visualization of the circulation pattern (2.3).